S$_N$2 versus E2 Competition of F$^-$ and PH$_2^-$ Revisited

Pascal Vermeeren,[#] Thomas Hansen,[#] Maxime Grasser, Daniela Rodrigues Silva, Trevor A. Hamlin,* and F. Matthias Bickelhaupt*

Cite This: *J. Org. Chem.* 2020, 85, 14087−14093

Read Online

ACCESS | Metrics & More | Article Recommendations | SI Supporting Information

ABSTRACT: We have quantum chemically analyzed the competition between the bimolecular nucleophilic substitution (S$_N$2) and base-induced elimination (E2) pathways for F$^-$ + CH$_3$CH$_2$Cl and PH$_2^-$ + CH$_3$CH$_2$Cl using the activation strain model and Kohn−Sham molecular orbital theory at ZORA-OLYP/QZ4P. Herein, we correct an earlier study that intuitively attributed the mechanistic preferences of F$^-$ and PH$_2^-$, i.e., E2 and S$_N$2, respectively, to a supposedly unfavorable shift in the polarity of the abstracted β-proton along the PH$_2^-$-induced E2 pathway while claiming that "*...no correlation between the thermodynamic basicity and E2 rate should be expected.*" Our analyses, however, unequivocally show that it is simply the 6 kcal mol^{-1} higher proton affinity of F$^-$ that enables this base to engage in a more stabilizing orbital interaction with CH$_3$CH$_2$Cl and hence to preferentially react via the E2 pathway, despite the higher characteristic distortivity (more destabilizing activation strain) associated with this pathway. On the other hand, the less basic PH$_2^-$ has a weaker stabilizing interaction with CH$_3$CH$_2$Cl and is, therefore, unable to overcome the characteristic distortivity of the E2 pathway. Therefore, the mechanistic preference of PH$_2^-$ is steered to the S$_N$2 reaction channel (less-destabilizing activation strain).
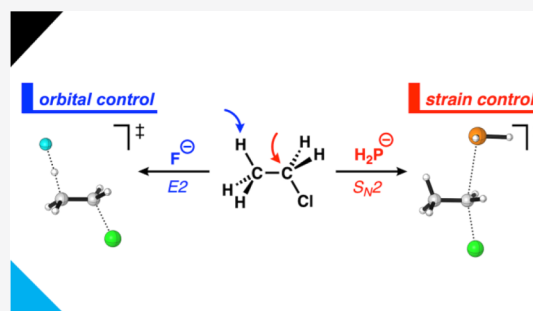
INTRODUCTION

The bimolecular nucleophilic substitution (S$_N$2) and base-induced bimolecular elimination (E2) reactions are two elementary reactions in the field of organic chemistry.[1,2] These two reactions are, in principle, always in competition with each other (Scheme 1), which might cause unwanted side

Scheme 1. Generic S$_N$2 and E2 Reactions
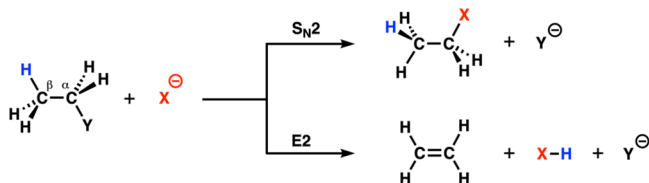
reactions and hampers the applicability of these reactions in synthetic chemistry. Moreover, the S$_N$2/E2 competition plays a paramount role in the development of modern mechanistic organic chemical insights.[3] Therefore, over the past decades, the S$_N$2/E2 competition has been extensively studied, both experimentally[4] and computationally.[5]

An important indicator of the reaction pathway preference is the basicity of the Lewis base, which is closely related to the proton affinity (PA). In general, a weak Lewis base (low proton affinity) will have a weak acid−base-like interaction with the substrate, and hence the mechanistic preference will be determined by the characteristic distortivity (i.e., degree of

activation strain) accompanying a reaction pathway. This factor is always more favorable (i.e., less destabilizing) for the less-distortive S$_N$2 pathway, making the Lewis base a nucleophile. In contrast, a strong interacting Lewis base (high proton affinity) is, due to its strong acid−base-like interaction with the substrate, able to overcome the highly destabilizing characteristic distortivity and favors the stronger interacting E2 pathway, reacting as a protophile.[6]

F$^-$ and PH$_2^-$ are ideal model Lewis bases that can be exploited to assess the competition between S$_N$2 and E2 pathways since they display opposing reactivity preferences,[7] even though it was believed that these two Lewis bases were essentially equal in terms of basicity (experimental PA: F$^-$ = 371.4 kcal mol^{-1}, PH$_2^-$ = 367.1 kcal mol^{-1}).[8,9] Scott Gronert concluded, in a previous study, that F$^-$ acts as a protophile and abstracts the β-proton via the E2 pathway, whereas PH$_2^-$ acts as a nucleophile and attacks at the α-carbon center following the S$_N$2 pathway.[7a] This selectivity was ascribed to the fact that, along the E2 pathway, proton transfer to the third-row Lewis base PH$_2^-$ involves a charge reorganization of the transferring hydrogen atom from protonic, when bonded to the

substrate, to hydridic, once it is coordinated to PH_2^-. Thus, Gronert states in this study: "*Intuitively, this shift in polarity [charge reorganization] should involve a significant [E2] barrier,*"[7a] which ultimately leads to a preference for the S_N2 pathway. In addition, the author emphasizes that "*...no correlation between thermodynamic basicity and E2 rate should be expected.*"[7a]

Here, we show that the rationale, proposed by Gronert,[7a] behind the opposing S_N2/E2 preferences of the Lewis bases F^- and PH_2^- is incorrect and that the observed selectivity does, on the contrary, find its origin in the difference in thermodynamic basicity. To this end, we have performed an in-depth computational study to unravel the physical mechanism behind the S_N2/E2 preferences of the Lewis bases F^- and PH_2^- with the model substrate chloroethane (CH_3CH_2Cl) (Scheme 2). The activation strain model (ASM)[10] in

Scheme 2. Schematic Overview of the Computationally Analyzed S_N2 and E2 Reactions of F^- (a) and PH_2^- (b) with Chloroethane 1
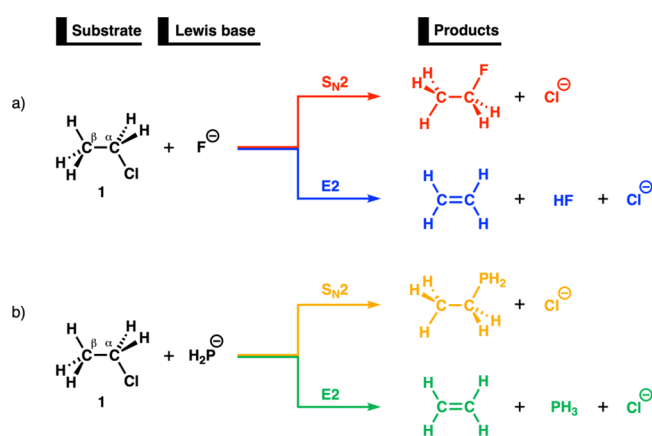
combination with Kohn–Sham molecular orbital (KS-MO)[11a] theory and the matching energy decomposition analysis (EDA)[11b,c] were employed to provide quantitative insight into the factor controlling the S_N2/E2 preference of the aforementioned reactions. This methodological approach facilitates the analysis of the potential energy surface and, more importantly, the activation barrier, by decomposing the total energy of the system into physically meaningful and easily interpretable terms, proving to be valuable for understanding the reactivity of, amongst others, nucleophilic substitution and elimination reactions.[12]

RESULTS AND DISCUSSION

The thermodynamic basicity of an anion in the gas phase is usually measured by means of its proton affinity (PA), which is the negative of the enthalpy change for a gas-phase reaction such as eq 1:

$$XH \rightarrow X^- + H^+ \tag{1}$$

where $X^- = F^-$ and PH_2^-. A high proton affinity indicates a stronger Lewis base and a weaker conjugated acid. The computed proton affinities (ΔH_{PA}) of the Lewis bases at ZORA-OLYP/QZ4P level are not similar. They, namely, differ by 6 kcal mol^{-1} (375.0 and 368.8 kcal mol^{-1}, F^- and PH_2^-, respectively), which is, as we will show later, large enough to significantly affect the thermodynamic basicity and hence the preferred reaction pathway. Note that our computed proton affinities compare well with previously reported theoretically[5] and experimentally[7,8] obtained proton affinities.

The reaction pathways of the bimolecular nucleophilic substitution (S_N2) and base-induced elimination (E2) reactions of Lewis bases F^- and PH_2^- with chloroethane (**1**), together with their transition state structures, are shown in Figure 1. In analogy with previous computational studies,[5f,g] we established that the F^- Lewis base has a strong preference
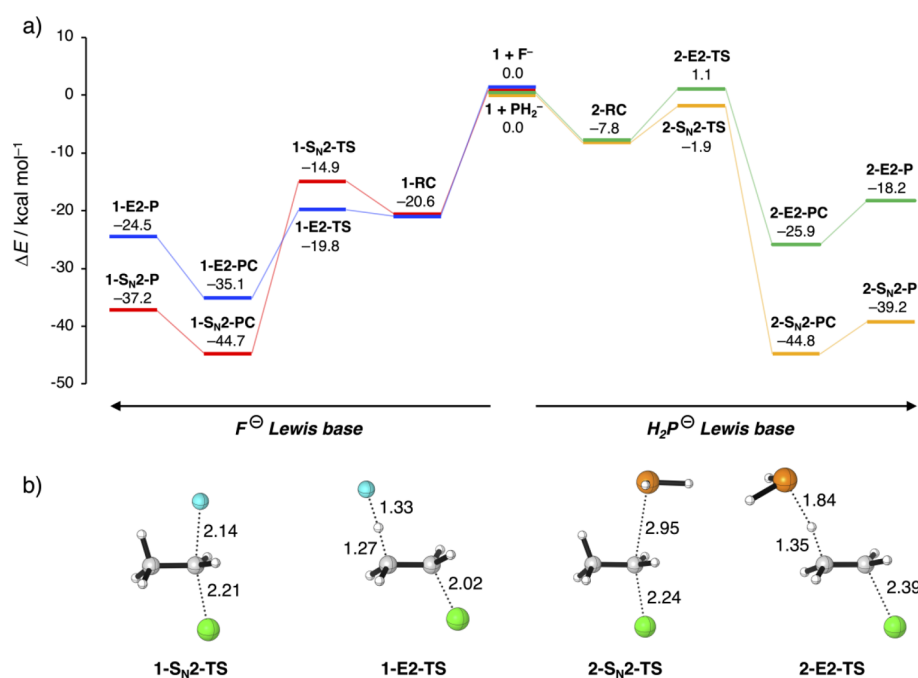

Figure 1. (a) Reaction profiles of the S_N2 and E2 reactions between **1** and the Lewis bases F^- and PH_2^- (in kcal mol^{-1}), computed at ZORA-OLYP/QZ4P. (b) Transition state structures with key bond lengths (in Å) for the S_N2 and E2 reactions between **1** and the Lewis bases F^- and PH_2^-.

for the E2 reaction pathway, whereas the S_N2 pathway is slightly favored by the PH_2^- Lewis base. The E2 reaction pathway for the attack with the F^- Lewis base proceeds with an activation barrier that is almost 5 kcal mol^{-1} lower in energy than for the S_N2 reaction pathway, but the latter results in a more stable product complex. For the reaction with PH_2^-, both the activation barrier and the product complex are in favor of the S_N2 reaction pathway. These findings are in line with Ren, Wong, and co-workers, who also found that F^- prefers the E2 reaction channel, whereas PH_2^- reacts via an S_N2 channel.[7b] These results already show that the differences in the proton affinities of the herein studied Lewis acids are significant enough to alter the preferred reaction pathway.

To gain quantitative insight into the physical factors leading to the preferred reaction pathway (S_N2 or E2), we turned to the activation strain model (ASM) of reactivity.[10] First, we focus on the reaction with the strong Lewis base F^-, as shown in Figure 2a. The previously mentioned preference for the E2 reaction pathway originates solely from a significantly more stabilizing interaction energy, which is strong enough to overcome the accompanied highly destabilizing characteristic distortivity (activation strain) associated with this pathway. Note that the distortion, characteristic of the E2 reaction, is inherently higher than that for the S_N2 reaction because along the former reaction pathway two bonds of **1** ($C^\alpha-Cl$ and $C^\beta-H$) are being broken, while for the latter, only one ($C^\alpha-Cl$) is being broken.[6] To understand why the E2 pathway goes with a stronger interaction, we employed a canonical energy decomposition analysis (EDA).[11b,c] We found that the significantly more stabilizing orbital interactions, together with the more favorable electrostatic interaction, for the E2 reaction pathway leads to the observed lower activation barrier of this reaction compared to the S_N2 analog (Figure 2b).

The origin of the more stabilizing orbital interactions of the E2 reaction pathway can be analyzed and explained by means of a Kohn−Sham molecular orbital analysis (KS-MO).[11a,13] We have quantified the key occupied−unoccupied orbital interaction between the $2p$ atomic orbital (AO) of F^- ($HOMO_{F^-}$) and the antibonding σ^*_{C-Cl} unoccupied orbital of **1** ($LUMO_1$) that participate in the acid−base-like interaction between the reactants at consistent geometries with a $C^\alpha\cdots Cl$ bond stretch of 0.404 Å (Figure 2c). The stronger orbital interaction of the E2 pathway is caused by both a smaller $HOMO_{F^-}-LUMO_{1,E2}$ energy gap, as a consequence of a more stable $LUMO_{1,E2}$, and a better orbital overlap, compared to the S_N2 pathway. The characteristic distortivity of both pathways has an immediate, but independent, impact on the electronic structure of **1**. The $LUMO_1$ has antibonding character not only in the $C^\alpha-Cl$ bond, but also in the $C^\beta-H$ bond. Thus, when both bonds are elongated, as a result of the characteristic distortion along the E2 pathway, the antibonding overlap of both bonds is reduced, which stabilizes, i.e., lowers the energy of, the $LUMO_{1,E2}$ and, therefore, makes the substrate more acidic.[5f,g,6] In comparison, the $LUMO_{1,SN2}$ benefits solely from the decreasing antibonding overlap of the $C^\alpha-Cl$ bond and, therefore, lowers to a lesser extent, making the substrate less acidic than along the E2 pathway. Furthermore, the more favorable orbital overlap of the E2 pathway is a direct response of the shorter distance between F^- and **1** compared to the S_N2 pathway. Thus, the strongly stabilizing interactions between F^- and **1** pushes the preference toward the pathway that involves the more destabilizing activation strain (E2 elimination).
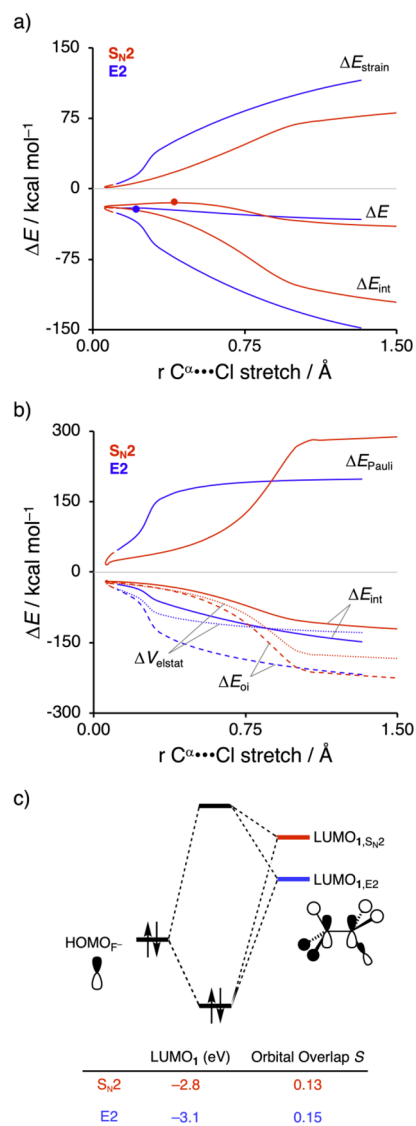
Figure 2. (a) Activation strain analysis and (b) energy decomposition analysis of the S_N2 and E2 reactions between **1** and F^-, where the energy values are projected on the $C^\alpha\cdots Cl$ bond stretch; (c) molecular orbital diagram of the most important $HOMO_{F^-}-LUMO_1$ orbital interaction computed at consistent geometries with a $C^\alpha\cdots Cl$ bond stretch of 0.404 Å, computed at ZORA-OLYP/QZ4P.

Next, we turn to the S_N2 and E2 reactions between PH_2^- and **1**, where the S_N2 pathway is now favored over the E2 pathway. By applying the ASM, we found that in contrast with the reactions involving F^-, the interaction between the weaker Lewis base PH_2^- and the substrate is not able to overcome the higher activation strain characteristic for the E2 reaction (Figure 3a). Our EDA clearly shows that all energy terms of the S_N2 and E2 pathways are at the early stage of the reaction nearly superimposed (Figure 3b), resulting in an identical interaction energy. Thus, the preference for the S_N2 pathway is exclusively governed by the less destabilizing characteristic distortion, which, in turn, is a result of only one bond-breaking event ($C^\alpha-Cl$) compared to the E2 pathway, where two bonds of **1** are being broken ($C^\alpha-Cl$ and $C^\beta-H$).

At last, we wish to understand why the E2 reaction between F^- and **1** goes with a more stabilizing interaction energy compared to the PH_2^- analog. The difference between the two
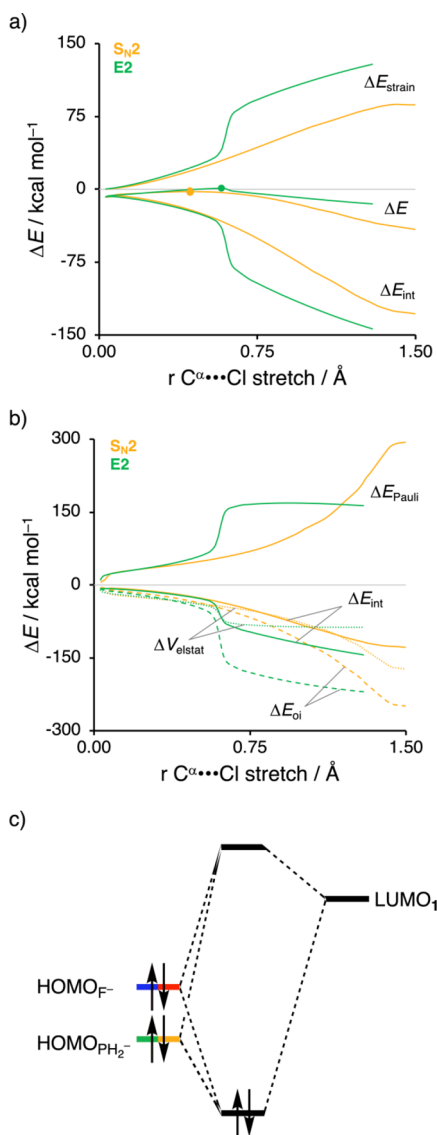
Figure 3. (a) Activation strain analysis and (b) energy decomposition analysis of the S_N2 and E2 reactions between **1** and PH_2^-, where the energy values are projected on the $C^\alpha \cdots Cl$ bond stretch, computed at ZORA-OLYP/QZ4P. (c) Schematic molecular orbital diagram of the most important $HOMO_{X^-} - LUMO_1$ orbital interaction, where $X^- = F^-$ or PH_2^-.

Lewis bases can be ascribed to the differences in the orbital energy of their interacting lone pair HOMOs, which, in turn, translates into the intrinsic differences in acid−base-like interactions with the substrate. As shown in Figure 3c, the HOMO of F^- is higher in energy (i.e., less stable) than the corresponding $HOMO_{PH2^-}$, making the former a stronger Lewis base. This can be explained by the size of the orbitals of the Lewis base. F^- has a less stable HOMO due to the compactness of fluorine AOs, which experiences more destabilizing Coulomb repulsion between the electrons compared to the heavier and larger $HOMO_{PH2^-}$. As a result, the more basic Lewis base F^- is able to form a stronger acid−base-like complex with the previously mentioned more acidic E2 substrate (i.e., small $HOMO_{F^-} - LUMO_1$ gap), compared to the weaker base PH_2^- (i.e., large $HOMO_{PH2^-} - LUMO_1$ gap), and is, therefore, able to generate a sufficiently stabilizing interaction with the substrate to overcome the characteristic

distortion accompanying the E2 reaction pathway. Thus, interestingly, while PH_2^- indeed reacts via a higher activation barrier than F^-, as found by Scott Gronert,[7a] this has little to do with the *shift in polarity* (i.e., charge reorganization), but instead with the fact that PH_2^- is a weaker Lewis base and hence interacts in a less favorable manner with the substrate.

CONCLUSIONS

In the competition between bimolecular nucleophilic substitution (S_N2) and base-induced elimination (E2) reactions, the mechanistic preference is influenced by many factors, including the basicity of the Lewis base. In this work, we have corrected the rationale postulated by Scott Gronert[7a] that explained the opposing S_N2/E2 preferences of the Lewis bases F^- and PH_2^- to the charge reorganization of the transferring hydrogen atom upon reacting with PH_2^- and, explicitly, not by their differences in thermodynamic basicity. Alternatively, we found that these two classical Lewis bases do exhibit sufficiently different proton affinities, which ultimately leads to opposite mechanistic preferences; namely, the stronger Lewis base F^- prefers to react via the E2 pathway, while the weaker Lewis base PH_2^- follows the S_N2 pathway.

Our activation strain analysis revealed the underlying physical mechanisms behind the S_N2/E2 preferences of the herein studied systems. We found that the E2 preference for the more basic Lewis base F^- originates from a stronger interaction with the substrate, as a result of more stabilizing orbital interactions, which is able to overcome the more destabilizing activation strain that goes with the high characteristic distortion of the E2 pathway. This higher extent of distortion also causes the substrate's LUMO to drop further and become more stable along the E2 pathway than the S_N2 pathway. In other words, the substrate becomes effectively more acidic along the E2 pathway and engages in a stronger orbital interaction with the Lewis base, due to a smaller $HOMO_{F^-} - LUMO_{1,E2}$ energy gap, compared to the S_N2 pathway.

This behavior is different for PH_2^-. Here, the weaker Lewis base PH_2^- interacts in a less stabilizing fashion with the substrate and is, thus, not able to overcome the highly destabilizing characteristic activation strain of the E2 reaction. Therefore, the preference for the S_N2 pathway is exclusively governed by the less destabilizing activation strain. The striking difference in the strength of the interaction between the two herein studied Lewis bases and the substrate can be ascribed to the differences in the orbital energy of their interacting lone pair HOMOs, which also explains the difference in thermodynamic basicity. The stronger base F^- (higher-energy HOMO) interacts more strongly with the more acidic substrate along the E2 reaction pathway, forming a more stable acid−base-like complex, compared to the much weaker base PH_2^- (lower-energy HOMO); hence, it is able to overcome the characteristic distortion accompanying the E2 reaction pathway.

METHODS

Computational Details. All density functional theory (DFT) calculations were performed using the Amsterdam Density Functional (ADF2018.105) software package.[14] The generalized gradient approximation (GGA) exchange-correlation functional OLYP was used for all computations, which consists of the optimized exchange (OPTX) functional proposed by Handy and co-workers[15a], and the Lee−Yang−Parr (LYP) correlation functional.[15b] Our previous

benchmark studies have shown that OLYP reproduces S_N2 barriers from highly correlated ab initio within only a few kcal mol^{-1}.[16] Scalar relativistic effects are accounted for using the zeroth-order regular approximation (ZORA).[17] The basis set used, denoted as QZ4P, is of quadruple-ζ quality for all atoms and has been improved by four sets of polarization functions.[18] This large basis set is required for small anionic species such as F^-.[16b] The accuracies of the fit scheme (Zlm fit) and the integration grid (Becke grid) were, for all calculations, set to VERYGOOD.[19] No symmetry constraints were used during the analyses. All calculated stationary points have been verified by performing a vibrational analysis calculation,[20] to be energy minima (no imaginary frequencies) or transition states (only one imaginary frequency). The character of the normal mode associated with the imaginary frequency of the transition state has been inspected to ensure that it is associated with the reaction of interest. The potential energy surfaces of the studied S_N2 and E2 reactions were obtained by performing intrinsic reaction coordinate (IRC) calculations,[21] which, in turn, were analyzed using the PyFrag 2019 program.[22] The optimized structures were illustrated using CYLview.[23]

Thermochemistry. Bond enthalpies, i.e., proton affinities (PA), are calculated at 298.15 K and 1 atm (ΔH_{PA}) from electronic bond energies (ΔE) and vibrational frequencies using standard thermochemistry relations for an ideal gas [eq 2].[24]

$$\Delta H_{PA} = \Delta E + \Delta E_{trans,298} + \Delta E_{rot,298} + \Delta E_{vib,0} + \Delta(\Delta E_{vib,0})_{298}$$
$$+ \Delta(pV) \qquad (2)$$

Here, $\Delta E_{trans,298}$, $\Delta E_{rot,298}$, and $\Delta E_{vib,0}$ are the differences between the complex (i.e., HF and PH_3, the protonated Lewis bases) and the separate species (i.e., $H^+ + F^-$ and $H^+ + PH_2^-$, the proton and the Lewis base) in translational, rotational, and zero-point vibrational energy, respectively. The last term, $\Delta(\Delta E_{vib,0})_{298}$, is the change in the vibrational energy difference when going from 0 to 298.15 K. The molar work term $\Delta(pV)$ is $(\Delta n)RT$, where $\Delta n = +1$, for one complex (HF or PH_3) dissociating into two separate species, namely the H^+ and Lewis base.

Activation Strain and Energy Decomposition Analysis. The activation strain model (ASM) of chemical reactivity,[10] also known as the distortion/interaction model,[25] is a fragment-based approach in which the potential energy surface (PES) can be described with respect to, and understood in terms of the characteristics of, the reactants. It considers the rigidity of the reactants and to which extent they need to deform during the reaction plus their capability to interact with each other as the reaction proceeds. With the help of this model, we decompose the total energy, $\Delta E(\zeta)$, into the strain and interaction energy, $\Delta E_{strain}(\zeta)$ and $\Delta E_{int}(\zeta)$, respectively, and project these values onto the reaction coordinate ζ [eq 3].

$$\Delta E(\zeta) = \Delta E_{strain}(\zeta) + \Delta E_{int}(\zeta) \qquad (3)$$

In this equation, the strain energy, $\Delta E_{strain}(\zeta)$, is the penalty that needs to be paid to deform the reactants from their equilibrium to the geometry they adopt during the reaction at point ζ of the reaction coordinate. On the other hand, the interaction energy, $\Delta E_{int}(\zeta)$, accounts for all the chemical interactions that occur between these two deformed reactants along the reaction coordinate.

The interaction energy between the deformed reactants can be further analyzed in terms of quantitative Kohn−Sham molecular orbital (KS-MO) theory together with a canonical energy decomposition analysis (EDA).[11] The EDA decomposes the $\Delta E_{int}(\zeta)$ into the following three energy terms [eq 4]:

$$\Delta E_{int}(\zeta) = \Delta V_{elstat}(\zeta) + \Delta E_{Pauli}(\zeta) + \Delta E_{oi}(\zeta) \qquad (4)$$

Herein, $\Delta V_{elstat}(\zeta)$ is the classical electrostatic interaction between the unperturbed charge distributions of the (deformed) reactants and is usually attractive. The Pauli repulsion, $\Delta E_{Pauli}(\zeta)$, includes the destabilizing interaction between the fully occupied orbitals of both fragments due to the Pauli principle. The orbital interaction energy, $\Delta E_{oi}(\zeta)$, accounts for, amongst others, charge transfer between the fragments, such as HOMO−LUMO interactions.

In the herein presented activation strain and accompanied energy decomposition diagrams, the energy terms are projected onto the carbon−leaving group (C^α−Cl) distance. This critical reaction coordinate undergoes a well-defined change during the reaction from the reactant complex via the transition state to the product and is shown to be a valid reaction coordinate for studying S_N2/E2 reactions.[12]

■ ASSOCIATED CONTENT

ⓢ Supporting Information

The Supporting Information is available free of charge at https://pubs.acs.org/doi/10.1021/acs.joc.0c02112.

> Additional computational results; and Cartesian coordinates, energies, and number of imaginary frequencies of all stationary points (PDF)

■ AUTHOR INFORMATION

Corresponding Authors

Trevor A. Hamlin − Department of Theoretical Chemistry, Amsterdam Institute of Molecular and Life Sciences (AIMMS), Amsterdam Center for Multiscale Modeling (ACMM), Vrije Universiteit Amsterdam, 1081 HV Amsterdam, The Netherlands; ⓞ orcid.org/0000-0002-5128-1004; Email: t.a.hamlin@vu.nl

F. Matthias Bickelhaupt − Department of Theoretical Chemistry, Amsterdam Institute of Molecular and Life Sciences (AIMMS), Amsterdam Center for Multiscale Modeling (ACMM), Vrije Universiteit Amsterdam, 1081 HV Amsterdam, The Netherlands; Institute for Molecules and Materials (IMM), Radboud University, 6525 AJ Nijmegen, The Netherlands; ⓞ orcid.org/0000-0003-4655-7747; Email: f.m.bickelhaupt@vu.nl

Authors

Pascal Vermeeren − Department of Theoretical Chemistry, Amsterdam Institute of Molecular and Life Sciences (AIMMS), Amsterdam Center for Multiscale Modeling (ACMM), Vrije Universiteit Amsterdam, 1081 HV Amsterdam, The Netherlands

Thomas Hansen − Department of Theoretical Chemistry, Amsterdam Institute of Molecular and Life Sciences (AIMMS), Amsterdam Center for Multiscale Modeling (ACMM), Vrije Universiteit Amsterdam, 1081 HV Amsterdam, The Netherlands; Leiden Institute of Chemistry, Leiden University, 2333 CC Leiden, The Netherlands; ⓞ orcid.org/0000-0002-6291-1569

Maxime Grasser − Department of Theoretical Chemistry, Amsterdam Institute of Molecular and Life Sciences (AIMMS), Amsterdam Center for Multiscale Modeling (ACMM), Vrije Universiteit Amsterdam, 1081 HV Amsterdam, The Netherlands

Daniela Rodrigues Silva − Department of Theoretical Chemistry, Amsterdam Institute of Molecular and Life Sciences (AIMMS), Amsterdam Center for Multiscale Modeling (ACMM), Vrije Universiteit Amsterdam, 1081 HV Amsterdam, The Netherlands; Departamento de Química, Universidade Federal de Lavras, Lavras, Minas Gerais 37200-900, Brazil

Complete contact information is available at:
https://pubs.acs.org/10.1021/acs.joc.0c02112

Author Contributions

#P.V. and T.H. contributed equally to this work.

■ REFERENCES

(1) (a) Smith, M. B.. *March's Advanced Organic Chemistry: Reactions, Mechanisms, and Structure*; 7th ed., Wiley: New York, 2013. (b) Carey, F. A.; Sundberg, R. J. *Advanced Organic Chemistry, Part A*; 5th ed., Springer: New York, 2007.

(2) Hamlin, T. A.; Swart, M.; Bickelhaupt, F. M. Nucleophilic Substitution (S_N2): Dependence on Nucleophile, Leaving Group, Central Atom, Substituents, and Solvent. *ChemPhysChem* **2018**, *19*, 1315−1330.

(3) Lowry, T. H.; Richardson, K. S. *Mechanism and Theory in Organic Chemistry*, 3rd ed., Harper and Row: New York, 1987.

(4) See, for instance (a) DePuy, C. H.; Bierbaum, V. M. Gas-Phase Elimination Reactions of Ethers Induced by Amide and Hydroxide Ions. *J. Am. Chem. Soc.* **1981**, *103*, 5034−5038. (b) DePuy, C. H.; Beedle, E. C.; Bierbaum, V. M. Reactions of Cyclic Ethers with Amide and Hydroxide Ions in the Gas Phase. *J. Am. Chem. Soc.* **1982**, *104*, 6483−6488. (c) Jones, M. E.; Ellison, G. B. A Gas-Phase E2 Reaction: Methoxide Ion and Bromopropane. *J. Am. Chem. Soc.* **1989**, *111*, 1645−1654. (d) DePuy, C. H.; Gronert, S.; Mulin, A.; Bierbaum, V. M. Gas-Phase S_N2 and E2 Reactions of Alkyl Halides. *J. Am. Chem. Soc.* **1990**, *112*, 8650−8655. (e) Lum, R. C.; Grabowski, J. J. Intrinsic Competition between Elimination and Substitution Mechanisms Controlled by Nucleophile Structure. *J. Am. Chem. Soc.* **1992**, *114*, 9663−9665. (f) Gronert, S.; Fagin, A. E.; Okamoto, K.; Mogali, S.; Pratt, L. M. Leaving Group Effects in Gas-Phase Substitutions and Eliminations. *J. Am. Chem. Soc.* **2004**, *126*, 12977−12983. (g) Gronert, S.; Fagin, A. E.; Wong, L. Direct Measurements of Deuterium Kinetic Isotope Effects in Anionic. Gas-Phase Substitution Reactions. *J. Am. Chem. Soc.* **2007**, *129*, 5330−5331.

(5) See, for instance (a) Minato, T.; Yamabe, S. Theoretical Studies on Gas-Phase Reactions of Fluoride Ion with Fluoroethance: E2 and S_N2 Reactions. *J. Am. Chem. Soc.* **1985**, *107*, 4621−4626. (b) Gronert, S.; Merrill, G. N.; Kass, S. R. Fluoride-Induced Elimination of Ethyl Fluoride. The Importance of High-Level Optimizations in ab Initio and DFT Studied. *J. Org. Chem.* **1995**, *60*, 488−489. (c) Gronert, S.; Kass, S. R. Theoretical Studies of Eliminations. 6. The Regiochemistry and Stereochemistry of the Gas-Phase Reactions of 3-Halocyclohexenes with Fluoride. An ad Initio Study. *J. Org. Chem.* **1997**, *62*, 7991−8000. (d) Gronert, S. Theoretical Studies of Elimination Reactions. 4. Gas Phase Reactions of F⁻ with Cyclopentyl and Cyclohexyl Chloride. Stereochemical Preferences of E2 Eliminations. *J. Org. Chem.* **1994**, *59*, 7046−7050. (e) Gronert, S.; Freed, P. Theoretical Studies of Eliminations. 5. Intermolecular vs Intramolecular Eliminations: An ab Initio Study of the Gas-Phase reaction between NH_2^- with $CH_3CH_2SCH_3$. *J. Org. Chem.* **1996**, *61*, 9430−9433. (f) Bickelhaupt, F. M.; Baerends, E. J.; Nibbering, N. M. M.; Ziegler, T. Theoretical Investigation on Base-Induced 1,2-Eliminations in the Model System Fluoride ion + Fluoroethane. The Role of the Base as a Catalyst. *J. Am. Chem. Soc.* **1993**, *115*, 9160−9173. (g) Bickelhaupt, F. M.; Baerends, E. J.; Anibbering, N. M. M. The Effect of Microsolvation on E2 and S_N2 Reactions: Theoretical Study of the Model System F⁻ + C_2H_5F + nHF. *Chem. − Eur. J.* **1996**, *2*, 196−207.

(6) Vermeeren, P.; Hansen, T.; Jansen, P.; Swart, M.; Hamlin, T. A.; Bickelhaupt, F. M. A Unified Framework for Understanding Nucleophilicity and Protophilicity in the $S_N2/E2$ Competition. *Chem. − Eur. J.* **2020**, DOI: 10.1002/chem.202003831.

(7) (a) Gronert, S. Theoretical Studies of Elimination Reactions. 1. Reactions of F⁻ and PH_2^- with CH_3CH_2C1. Competition between S_N2 and E2 Mechanisms for First- and Second-Row Nucleophiles. *J. Am. Chem. Soc.* **1991**, *113*, 6041−6048. (b) Wu, X.-P.; Sun, X.-M.; Wei, X.-G.; Ren, Y.; Wong, N.-B.; Li, W.-K. Exploring the Reactivity Trends in the E2 and S_N2 Reactions of X⁻ + CH_3CH_2Cl (X = F, Cl, Br, HO, HS, HSe, NH_2, PH_2, AsH_2, CH_3, SiH_3, and GeH_3). *J. Chem. Theory Comput.* **2009**, *5*, 1597−1606.

(8) (a) Holtz, D.; Beauchamp, J. L.; Eyler, J. R. Acidity, Basicity, and Ion-Molecule Reactions of Phosphine in the Gas Phase by Ion Cyclotron Resonance Spectroscopy. *J. Am. Chem. Soc.* **1970**, *92*, 7045−7055. (b) Ervin, K. M.; Lineberger, W. C. Photoelectron Spectroscopy of Phosphorus Hydride Anions. *J. Chem. Phys.* **2005**, *122*, 194303.

(9) Acree, Jr., W. E.; Chickos, J. S.. In *NIST Chemistry WebBook, NIST Standard Reference database Number 69*, Ed. Linstrom, P. J.; Mallard, W. G., National Institute of Standards and Technology, Gaithersburg MD.

(10) (a) Vermeeren, P.; van der Lubbe, S. C. C.; Fonseca Guerra, C.; Bickelhaupt, F. M.; Hamlin, T. A. Understanding Chemical Reactivity Using the Activation Strain Model. *Nat. Protoc.* **2020**, *15*, 649−667. (b) Bickelhaupt, F. M.; Houk, K. N. Analyzing Reaction Rates with the Distortion/Interaction-Activation Strain Model. *Angew. Chem., Int. Ed.* **2017**, *56*, 10070−10086; *Angew. Chem., Int. Ed.* **2009**, *129*, 10204−10221. (c) Bickelhaupt, F. M. Understanding Reactivity with Kohn−Sham Molecular Orbital Theory: E2−S_N2 Mechanistic Spectrum and Other Concepts. *J. Comput. Chem.* **1999**, *20*, 114−128.

(11) (a) Bickelhaupt, F. M.; Baerends, E. J. Kohn-Sham Density Functional Theory: Predicting and Understanding Chemistry. In *Reviews in Computational Chemistry*; Lipkowitz, K. B.; Boyd, D. B., Eds.; Wiley-VCH: New York, 2000; *15*, 1−86. (b) van Meer, R.; Gritsenko, O. V.; Baerends, E. J. Physical Meaning of Virtual Kohn-Sham Orbitals and Orbital Energies: An Ideal Basis for the Description of Molecular Excitations. *J. Chem. Theory Comput.* **2014**, *10*, 4432−4441. (c) Zhao, L.; von Hopffgarten, M.; Andrada, D. M.; Frenking, G. Energy Decomposition Analysis. *WIREs Comput. Mol. Sci.* **2018**, *8*, No. e1345.

(12) (a) Hamlin, T. A.; van Beek, B.; Wolters, L. P.; Bickelhaupt, F. M. Nucleophilic Substitution in Solution: Activation Strain Analysis of Weak and Strong Solvent Effects. *Chem. − Eur. J.* **2018**, *24*, 5927−5938. (b) Hansen, T.; Vermeeren, P.; Haim, A.; van Dorp, M. J. H.; Codée, J. D. C.; Bickelhaupt, F. M.; Hamlin, T. A. Regioselectivity of Epoxide Ring-Openings via S_N2 Reactions Under Basic and Acidic Conditions. *Eur. J. Org. Chem.* **2020**, 3822−3828. (c) Galabov, B.; Koleva, G.; Schaefer, H. F., III; Allen, W. D. Nucleophilic Influences and Origin of the S_N2 Allylic Effect. *Chem. − Eur. J.* **2018**, *24*, 11637−11648.

(13) Albright, T. A.; Burdett, J. K.; Wangbo, W. H. *Orbital Interactions in Chemistry*; 2nd ed., Wiley: New York, 2013.

(14) (a) te Velde, G.; Bickelhaupt, F. M.; Baerends, E. J.; Fonseca Guerra, C.; van Gisbergen, S. J. A.; Snijders, J. G.; Ziegler, T. Chemistry with ADF. *J. Comput. Chem.* **2001**, *22*, 931−967. (b) Fonseca Guerra, C.; Snijders, J. G.; te Velde, G.; Baerends, E. J. Towards an Order-N DFT Method. *Theor. Chem. Acc.* **1998**, *99*, 391−403. (c) *ADF2018.10S, SCM Theoretical Chemistry*; Vrije Universiteit, Amsterdam, The Netherlands, http://www.scm.com.

(15) (a) Handy, N. C.; Cohen, A. J. Left-right correlation energy. *Mol. Phys.* **2001**, *99*, 403−412. (b) Lee, C.; Yang, W.; Parr, R. G. Development of the Colle-Salvetti correlation-energy formula into a functional of the electron density. *Phys. Rev. B: Condens. Matter Mater. Phys.* **1988**, *37*, 785−−789.

(16) (a) Patrícia Bento, A.; Matthias Bickelhaupt, F.; Solà, M. E2 and S_N2 Reactions of X⁻ + CH_3CH_2X (X = F, Cl); an *ab initio* and DFT Benchmark Study. *J. Chem. Theory Comput.* **2008**, *4*, 929−940. (b) Swart, M.; Solà, M.; Bickelhaupt, F. M. Density Functional Calculations of E2 and S_N2 Reactions: Effects of the Choice of Method, Algorithm, and Numerical Accuracy. *J. Chem. Theory Comput.* **2010**, *6*, 3145−3152.

(17) van Lenthe, E.; Baerends, E. J.; Snijders, J. G. Relativistic total energy using regular approximations. *J. Chem. Phys.* **1994**, *101*, 9783−9792.

(18) van Lenthe, E.; Baerends, E. J. Optimized Slater-Type Basis Sets for the Elements 1−118. *J. Comput. Chem.* **2003**, *24*, 1142−1156.

(19) (a) Franchini, M.; Philipsen, P. H. T.; van Lenthe, E.; Visscher, L. Accurate Coulomb Potentials for Periodic and Molecular Systems through Density Fitting. *J. Chem. Theory Comput.* **2014**, *10*, 1994−2004. (b) Franchini, M.; Philipsen, P. H. T.; Visscher, L. The Becke Fuzzy Cells Integration Scheme in the Amsterdam Density Functional Program Suite. *J. Comput. Chem.* **2013**, *34*, 1819−1827.

(20) (a) Bérces, A.; Dickson, R. M.; Fan, L.; Jacobsen, H.; Swerhone, D.; Ziegler, T. An Implementation of the Coupled Perturbed Kohn-Sham Equations: Perturbation due to Nuclear Displacement. *Comput. Phys. Commun.* **1997**, *100*, 247−262. (b) Jacobsen, H.; Bérces, A.; Swerhone, D. P.; Ziegler, T. Analytic Second Derivatives of Molecular Energies: a Density Funtional Implementation. *Comput. Phys. Commun.* **1997**, *100*, 263−276. (c) Wolff, S. K. Analytical Second Derivatives in the Amsterdam Density Functional Package. *Int. J. Quantum Chem.* **2005**, *104*, 645−659.

(21) (a) Fukui, K. The Path of Chemical Reactions - the IRC Approach. *Acc. Chem. Res.* **1981**, *14*, 363−368. (b) Deng, L.; Ziegler, T.; Fan, L. A Combined Density Functional and Intrinsic Reaction Coordinate Study on the Ground State Energy Surface of H_2CO. *J. Chem. Phys.* **1993**, *99*, 3823−3835. (c) Deng, L.; Ziegler, T. The Determination of Intrinsic Reaction Coordinates by Density Functional Theory. *Int. J. Quantum Chem.* **1994**, *52*, 731−765.

(22) Sun, X.; Soini, T. M.; Poater, J.; Hamlin, T. A.; Bickelhaupt, F. M. PyFrag 2019−Automating the Exploration and Analysis of Reaction Mechanisms. *J. Comput. Chem.* **2019**, *40*, 2227−2233.

(23) Legault, C. Y., *CYLview, 1.0b*; Université de Sherbrooke, Canada, Sherbrooke, QC, 2009, http://www.cylview.org.

(24) (a) Atkins, P. W.; de Pauli, J. *Physical Chemistry*; 9th ed., Oxford University Press: Oxford, 2010. (b) Jensen, F. *Introduction to Computational Chemistry*; 2nd ed., Wiley: West Sussex, 2007.

(25) (a) Ess, D. H.; Houk, K. N. Distortion/Interaction Energy Control of 1,3-Dipolar Cycloaddition Reactivity. *J. Am. Chem. Soc.* **2007**, *129*, 10646−10647. (b) Ess, D. H.; Houk, K. N. Theory of 1,3-Dipolar Cycloadditions: Distortion/Interaction and Frontier Molecular Orbital Models. *J. Am. Chem. Soc.* **2008**, *130*, 10187−10198.